Received: 30 May 2022 | Revised: 18 July 2022 | Accepted: 22 July 2022

DOI: 10.1111/jfpp.16950

Journal of Food Processing and Preservation | Institute of Food Science + Technology | ifst | WILEY

ORIGINAL ARTICLE

Fabrication, characterization, and oxidative stability of perilla seed oil emulsions and microcapsules stabilized by protein and polysaccharides

Chuang Zhang[1,2] | Wenting Zhou[1] | Jiqian Xiang[3] | Hong Chen[4] | Siew Young Quek[1,5]

[1]Food Science, School of Chemical Sciences, The University of Auckland, Auckland, New Zealand

[2]College of Food Science and Technology, Nanjing Agricultural University, Nanjing, China

[3]Enshi Tujia & Miao Autonomous Prefecture Academy of Agricultural Sciences, Enshi, China

[4]Institute of Oil Crops Research, Chinese Academy of Agricultural Sciences, The Key Lab for Biological Sciences of Oil Crops, Ministry of Agriculture - Hubei Key Laboratory of Lipid Chemistry and Nutrition, Wuhan, China

[5]Riddet Institute, Centre of Research Excellence for Food Research, Palmerston North, New Zealand

Correspondence
Siew Young Quek, Food Science, School of Chemical Sciences, The University of Auckland, Auckland 1010, New Zealand.
Email: sy.quek@auckland.ac.nz

Abstract

Perilla oil (PO) has a high unsaturated fatty acids content that is easily oxidized, causing nutritional and functional losses. This study investigated the fabrication of PO in emulsion and microcapsules using whey protein isolate (WPI), gum acacia (GA), maltodextrin (MD), and OSA-starch as wall materials, aiming to improve the oxidative stability and functionality of the PO. The results showed that both OSA-starch stabilized emulsion and microcapsules exhibited slower increases in peroxide and *p*-anisidine values and a slower decrease in antioxidant capacity than those produced with WPI/GA, WPI/MD, and WPI/GA via complex coacervation. The microcapsules fabricated with OSA-starch gave a better polydispersity index, encapsulation efficiency, and oxidative stability than the other samples, suggesting effective protection against primary and secondary oxidation during storage. Moreover, the oxidation stability of the emulsions and microcapsules could be improved via complex coacervation, although this technique could result in a larger droplet size. Overall, this study contributed to the knowledge of PO emulsions and microcapsules fabrication using protein and polysaccharides and provided insights for improving PO's oxidative stability and functionality.

Novelty impact statement: Perilla oil can be successfully encapsulated by OSA-starch-based carriers. The study contributed to the knowledge of perilla oil emulsions and microcapsules fabrication and provided insights for improving perilla oil's oxidative stability and functionality.

1 | INTRODUCTION

Perilla fructescens, commonly known as perilla, is a member of the *Lamiaceae* family widely cultivated in East Asian countries such as China, Japan, and Korea. The leaves and seeds are the most applicable parts of *Perilla fructescens*. Perilla seed oil (PO) is considered a nutritional cooking oil and a food ingredient in seasoning, salad dressing, and dipping sauces. It contains a high percentage of unsaturated fatty acids, especially α-linolenic acid (ALA), an omega 3 fatty acid. ALA is the precursor of docosahexaenoic acid (DHA) and eicosapentaenoic acid (EPA) (Anderson & Ma, 2009), which have been linked to many health benefits such as anti-inflammatory, proper fetal development, cardio-protection, and brain damages prevention (Swanson et al., 2012; von Schacky, 2021). However, a high amount of unsaturated fatty acids in PO leads to poor stability and high susceptibility to oxidization, resulting in a loss of nutritional value and shorter shelf-life. Previous research demonstrated that PO is highly sensitive to oxidation as favored by its high concentration of ALA (Wang et al., 2010).

Oxidative instability is the main factor limiting the edible oil quality, including color, flavor, and nutritional components, directly related to economic, safety, and storage issues (Bae & Lee, 2008). Plant seed oils contain antioxidants such as phenolics and sterols (i.e., β-sitosterol, campesterol, stigmasterol, and avenasterol), which can prevent lipid oxidation and loss of color, flavor, and nutrition (Kozłowska et al., 2016). These bioactive compounds in PO need to be protected from degradation to achieve the desirable antioxidant performance. To address these issues, microencapsulation of PO into emulsion or microcapsule formats could be an effective way to reduce oxidative degradation and improve shelf-life stability.

The microencapsulation technique is now well developed and accepted for application in the food, chemical, cosmetic, and pharmaceutical industries. Various food ingredients that are susceptible to oxidative deterioration, including edible oils, colorants, enzymes, vitamins, and flavor compounds, have been encapsulated. A successful microencapsulation system is dependent on the choice of suitable wall material and encapsulation technique according to the specific core material. The selection of wall material is critical as it influences the properties of the resulted emulsion and microcapsules. Generally, an optimal wall material should have a good emulsifying property, high water solubility, suitable drying property, and low viscosity (Gharsallaoui et al., 2007).

Microencapsulation of PO has attracted some interest due to the high content of ALA in the oil. Several studies have compared the suitability of microencapsulation methods, that is, coacervation, spray drying, and freeze-drying (Chen et al., 2013, 2015) and the effect of wall materials (Han et al., 2016) on microencapsulation of PO. Those studies have mainly focused on the processing aspects and microcapsule properties without detailed investigations on the oil stability and emulsion characteristics before drying. More recent studies have looked at stabilizing PO using plant proteins (i.e., using black bean protein in a nanocomplex and soy protein isolate in nanoemulsion) (Han et al., 2021; Hu et al., 2020), and the use of chitosan, poly-L-lysine, sodium alginate, and for encapsulating PO in nanoliposomes (Zamani-Ghaleshahi et al., 2020).

When choosing a microencapsulation method for food ingredients, there are some critical factors to consider, including production cost, ease to scale up, and product stability. Considering the above factors, spray drying is a practical method for producing the microencapsulated PO. Common wall materials, including whey protein isolate (WPI), gum Arabic (GA), maltodextrin (MD), and octenyl succinic anhydride starch (OSA-starch) were chosen according to previous studies (Chen et al., 2013; Han et al., 2016) and their good emulsifying and film-forming properties (Gharsallaoui et al., 2007), availability and reasonable cost. Since many studies demonstrated that single wall material has a limited property to suffice all the requirements for microencapsulation (Sarabandi et al., 2017; Zhang, Khoo, et al., 2020), and considering the susceptibility of PO toward oxidation, a mixture of wall materials (which has not been attempted before) was explored to produce ideal protection for PO.

The objective of this study was to conduct systematic research on the fabrication of PO-containing emulsions and microcapsules using the abovementioned carbohydrates and protein to fill the research gaps. The physicochemical properties and oxidative stabilities of both the emulsions and spray-dried microcapsules were examined, emphasizing the effects of wall material types or combinations, core-to-wall ratio, and total solid content. The current research brought innovation by exploring the effect of various wall materials in the formation of emulsions and spray-dried microparticles containing PO. Furthermore, it evaluated the protection toward oxidative stability given by each wall material and their combinations. In addition, the findings provide fundamental knowledge of stabilizing perilla oil using spray drying microencapsulation, and promote the industrial development of perilla oil as a novel alternative edible oil. A complete study with the selected materials has not been published, to the best of our knowledge.

2 | MATERIALS AND METHODS

2.1 | Materials and reagents

Red seed PO was kindly provided by Enshi Qingjiang Biology Engineering Ltd. (Enshi, Hubei, China), and the fatty acid composition was determined (Table A1). Wall materials applied were as below: Whey protein isolate (WPI, WPI 895) from Fonterra Ltd. (Auckland, New Zealand), acacia gum (GA, instant gum BB) from Hawkins Watts Ltd. (Auckland, New Zealand), maltodextrin (MD, MD 1920) from Sherratt Ltd. (Auckland, New Zealand) and OSA-starch (HI-CAP® 100) from Ingredion China Ltd. (Shanghai, China). Chemicals including Supelco 37 Component FAME Mix, biphenyl, activated carbon, *p*-anisidine, 2,2-diphenyl-1-picrylhydrazyl (DPPH), and 6-hydroxy-2,5,7,8-tetramethylchroman-2-carboxylic acid (Trolox) were purchased from Sigma-Aldrich (St. Louis, MO, USA). Potassium hydroxide, potassium chloride, isopropanol, potassium iodide, sodium sulfite, sodium thiosulfate, and ethanol absolute were bought from ECP Ltd. (Auckland, New Zealand). Other chemicals were supplied as follows: boron trifluoride methanol complex solution (Riedel-de Haën™) and *n*-hexane (B&J Brand™) from Honeywell International Inc. (Charlotte, NC, USA), chloroform from Loba Chemie Pvt. Ltd. (Colaba, Mumbai, India) and isooctane from Ajax Finechem Pty Ltd. (Taren Point, NSW, Australia). All chemicals used were of analytical grade (AR). Ultrapure water was used in the experiments.

2.2 | Preparation of emulsions and microcapsules

2.2.1 | Preparation of emulsion

The oil-in-water (O/W) emulsions were prepared by encapsulating the core material (PO) into different wall materials. The wall materials were dissolved in the ultrapure water as the aqueous phase, and mixed with the PO to achieve a core-to-wall material ratio of 1:3 and 1:4 (w/w) and a final total solid content of 15 or 30% (w/w). The composition of all emulsions is shown in Table A2.

2.2.1.1 | *Preparation of aqueous phase*

Different wall materials required a slightly different preparation procedure. For preparing the WPI/GA and WPI/MD aqueous phase, the wall materials were dissolved in ultrapure water according to the proportion as shown in Table A2. The mixture was then stirred at 55°C for 1 h and left overnight at room temperature (22°C) for better dispersion. For OSA-starch, the aqueous phase was prepared by dissolving OSA-starch in ultrapure water according to the proportion as shown in Table A2. The mixture was stirred at 80°C for 1 h and was left stirring overnight at room temperature to ensure complete dissolution.

2.2.1.2 | *Preparation of emulsion via homogenization*

The core material (PO) was added into the aqueous solution as prepared above and stirred using a high-speed mixer (model: L5T, Silverson Machines Inc., East Longmeadow, MA, USA) at 3000 rpm for 10 min to achieve a crude emulsion, followed by passing through a pneumatic microfluidizer (model: HC-2000, Microfluidics, Newton, MA, USA) at 10,000 psi with two passes to obtain the final O/W emulsion.

2.2.1.3 | *Preparation of emulsion via complex coacervation*

Two samples (Table A2) were prepared via complex coacervation using WPI/GA as wall materials. Optimization of the coacervation for optimum pH value and WPI-to-GA ratio was conducted according to Eratte et al. (2014). From the results (Figure 1a), WPI-to-GA ratio of 3:1 and pH value of 4.36 (adjusted by citric acid) was selected for preparing the emulsions.

2.2.2 | Spray-dried microcapsules

The PO microcapsules were prepared by spray drying using a Büchi mini spray dryer (model: B-191, Büchi Laboratoriums-Technik, Flawil, Switzerland). The O/W emulsions, namely WG14, CWG14, WM14, OSA13, OSA14, and the emulsion OSA14 with a higher solid content of 30% (OSA14-30) (Table A2) were used as the feed solutions to produce the spray-dried microcapsules. Spray drying was performed at an inlet temperature of 180°C, pump capacity of 25%, aspirator rate of 75%, and gas nitrogen flow rate of 600 L/h. Powders in the collection vessel were used for further analyses.

2.3 | Extraction of oil from emulsion

The PO was extracted from the emulsion, according to Katvi (2005). Briefly, approximately 100 ml of *n*-hexane and 80 ml of isopropanol were transferred into a 500 ml separatory funnel containing 50 ml of emulsion sample. The mixture was shaken immediately for 2 min to prevent further emulsification. Then, ultrapure water (100 ml) was added to facilitate the separation of the aqueous and organic phases. The upper organic layer in the separatory funnel was transferred into a 250 ml round-bottom flask. Extraction was repeated for the remaining aqueous solution. The organic phase was collected and recovered using rotary evaporation at 30°C until almost dry. The residue was further flushed to dryness by nitrogen for 10 to 20 min. The extracted oil was transferred into a small centrifuge tube and kept at −80°C for further analysis.

2.4 | Fatty acids composition

The fatty acid composition was determined by converting fatty acids to fatty methyl esters (FAMEs) through alkaline transmethylation, followed by gas chromatography–mass spectrometry (GC–MS) analysis (Gamazo-Vázquez et al., 2003; Yi et al., 2014). Briefly, 25 mg of PO was placed into a 15 ml centrifuge tube, and 1.5 ml of 0.5 M KOH in methanol solution was added. The tube was then purged with nitrogen and incubated in a water bath at 90°C for 5 min. After cooling down, 2 ml of boron trifluoride methanol solution was added into the tube, and the content was mixed thoroughly using a Vortex (Vortexer, Heathrow Scientific, IL, USA). Subsequently, the tube was incubated at 90°C for 30 min, followed by adding 5 ml saturated KCl and 2 ml *n*-hexane solutions. The content was mixed thoroughly and centrifuged at 3000 rpm for 10 min. The supernatant containing FAMEs was carefully collected and diluted 50 times using *n*-hexane. An aliquot of 900 µl was then transferred into a GC vial and spiked with 100 µl of biphenyl (100 mg/L in *n*-hexane, internal standard) for GC–MS (Agilent Technologies, Santa Clara, CA, USA) analysis. The temperature program was set as follows: 45°C for 5 min, ramped to 200°C at 10°C/min, and finally increased to 230°C for 8 min at 3°C/min. An aliquot of 1 µl was injected into the instrument under a split ratio of 1:10. High-purity helium was used as the carrier gas with a flow rate set at 3.2 ml/min. The mass spectrometer was operated under the electron impact (EI) mode at 70 eV with a full scan from *m/z* 35 to 500. The FAMEs were quantitated using calibration curves established by a serial dilution of the Supelco 37 Component FAME Mix standard using *n*-hexane.

2.5 | Emulsion droplet size and size distribution

Oil droplets' size and size distribution in emulsions were determined using a Zetasizer Nano ZS (Malvern Panalytical Ltd., Malvern, UK). The emulsions were diluted by ultrapure water for 50 times before measurement. An aliquot of 1 ml diluted emulsion was added into the cuvette, and measurement was taken for 13 to 18 runs each time. The average droplet size and polydispersity index (PDI) were obtained via the size distribution curve by interpreting the diffraction patterns.

2.6 | Zeta-potential

The zeta-potential of the emulsions was determined using a Zetasizer Nano ZS instrument (Malvern Panalytical Ltd.). The diluted emulsion (from Section 2.5) was injected into a capillary cell (Malvern Panalytical Ltd.). The measurement was conducted with 50 runs for each time.

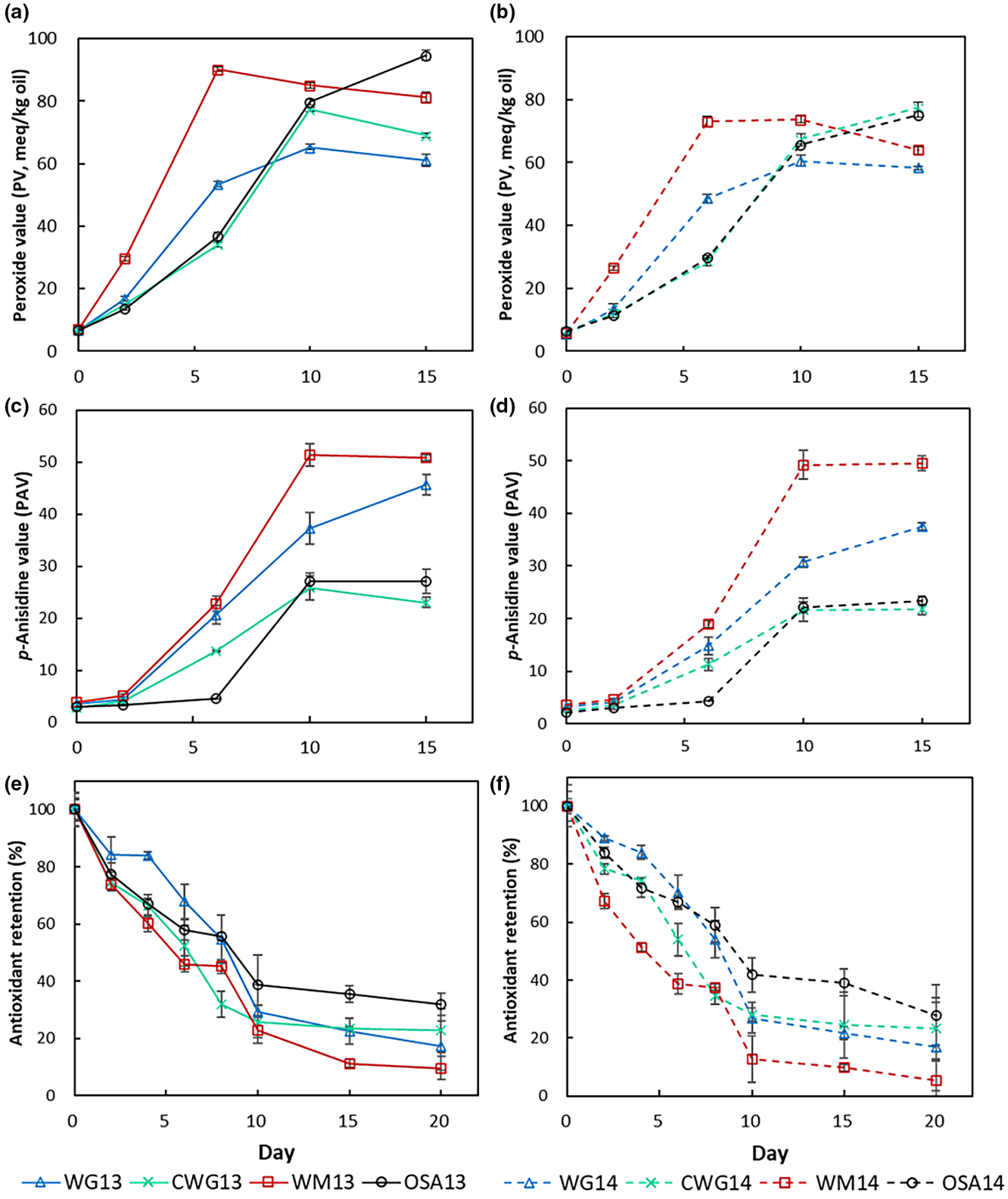

FIGURE 1 Oxidative stability of emulsions during storage. (a) and (b) for peroxide value; (c) and (d) for *p*-anisidine value; (e) and (f) for antioxidant retention.

2.7 | Oxidative stability

2.7.1 | Peroxide value

The peroxide value (PV) was determined using the iodometric titration method according to the American Oil Chemists' Society Official Method Cd 8-53 (AOCS, 1998) with modification. Briefly, 0.1 g of oil was weighed and transferred into a 50 ml Erlenmeyer flask and then dissolved in 1.5 ml of acetic acid-chloroform (3:2, v/v) solution with swirling. An aliquot of 25 µl of saturated potassium iodide (KI) solution was added and shaken for 1 min to achieve complete oxidation. Then, 1.5 ml of ultrapure water was immediately dispersed into the mixture followed by the addition of 1% (w/v) starch solution (2–3 drops). The complex became dark blue in color, and it was titrated with 0.1 M sodium thiosulfate ($Na_2S_2O_3$) with constant shaking until the dark blue color disappeared completely. The blank experiment was conducted without the addition of PO. The PV was calculated and expressed as peroxide milliequivalents per kilogram of oil (meq/kg).

$$\mathrm{PV\,(meq/kg)} = \frac{\mathrm{ml\ of\ Na2S2O3} \times M \times 1000}{\mathrm{the\ amount\ of\ PO\ (g)}} \quad (1)$$

where M is the molarity of $Na_2S_2O_3$ solution (0.1 mol/L).

2.7.2 | *p*-anisidine value

The *p*-anisidine value (PAV) was determined according to the AOCS Office Method Cd 18–90 (AOCS, 2009). Briefly, 50 mg of PO was weighed into a 25 ml volumetric flask and diluted with 2,2,4-trimethylpentane (isooctane) solution to the volume. The absorbance (A_b) of the oil solution was measured at 350 nm, using isooctane solution as the blank. Five milliliters of the oil-isooctane solution was transferred into a tube (labeled as tube A) and 5 ml of the isooctane was transferred into another tube (tube B). One milliliter of *p*-anisidine reagent solution (2.5 g/L) was added into tube A and B to react for 10 min, respectively. The absorbance (A_s) of the solution in tube A was measured at 350 nm using the solution in tube B as the blank. The PAV was calculated according to Equation 2 and expressed as the amount of secondary oxidation products (e.g., ketones and aldehydes) of the oils.

$$\mathrm{PAV} = \frac{25 \times (1.2As - Ab)}{\mathrm{mass\ of\ the\ oil\ (g)}} \quad (2)$$

2.7.3 | Antioxidant capacity

The antioxidant capacity was determined using the DPPH radical scavenging activity, according to Chen et al. (2019). Briefly, 10 µl of appropriately diluted sample was added into the 96-well plate. Then, 200 µl of DPPH solution (0.1 mM) was added and left for reaction (1 h in the dark). The absorbance of the sample was determined at 517 nm using a plate reader (EL 340, Bio-Tek Instruments Inc., Winooski, VT, USA). Trolox solutions with different concentrations (0.01, 0.02, 0.04, 0.08, 0.1, 0.2, and 0.4 mM prepared in ethanol) were used to construct a standard curve. The antioxidant capacity was expressed as mM Trolox equivalent per liter (mM TE/L) of samples.

2.8 | Characterization of spray-dried microcapsules

2.8.1 | Moisture content and water activity

The moisture content was determined gravimetrically by drying in an oven at 105°C until a constant weight was obtained. The water activity (a_w) was determined using a water activity analyzer (model: TH-500, Novasina Inc., Lachen, Switzerland), operating at 25°C.

2.8.2 | Bulk and tapped density

The bulk (ρB), tapped (ρT) densities, and flowability were determined according to Sarabandi et al. (Sarabandi et al., 2017) with modification. Briefly, 1 g of spray-dried powder was weighed (m_0) and gently loaded into a 10 ml glass-graduated cylinder. The volume (v_b) of powder was recorded, and the ρB was calculated according to Equation (3). Then, the cylinder was tapped on a flat surface until a constant volume (v_t) was achieved. The ρT was calculated according to Equation (4). The flowability of powder was described using the Carr's index (Equation 5), which indicated a fluid power with the value <25%, otherwise a cohesive powder.

$$\rho\mathrm{B} = m_0 / v_b \quad (3)$$

$$\rho\mathrm{T} = m_0 / v_t \quad (4)$$

$$\mathrm{Carr's\ index\ (\%)} = \frac{\rho\mathrm{T} - \rho\mathrm{B}}{\rho\mathrm{T}} \times 100\% \quad (5)$$

2.8.3 | Morphological observation

The microstructures of microcapsules were observed by a scanning electron microscope (SEM) (model: FEI Quanta 200 F, Hillsboro, Oregon, USA). A small amount of sample was fixed on a stub using a double-sided conducting carbon tape, followed by sputter coating with palladium (model: Quorum Q150 RS, Laughton, East Sussex, UK). The SEM was operated at a voltage of 10 kV and 0.7 Torr pressure under magnifications of 2500, 6000, and 12,000 times.

2.8.4 | Surface oil concentration

The amount of unencapsulated oil remaining at the microcapsule's surface was determined according to Tan et al. (2005) with

modification. Briefly, 1 g of powder sample was dispersed in a 10 ml *n*-hexane and shaken by a Vortex mixer for 10 s to extract the surface oil. The mixture was then filtered through a filter paper and powder was collected from the filter. After that, the powder was rinsed using 5 ml of *n*-hexane for two times. The filtrate containing extracted oil was transferred into a weighed round-bottom flask (W_1) followed by rotary evaporation. The solvent residue was removed by flushing with nitrogen for 10 min and the final weight (W_2) was recorded. The surface oil content was calculated as below:

$$\text{Surface oil}\,(\%) = \frac{(W2 - W1)\,(\text{g})}{\text{mass of the powder sample}\,(\text{g})} \times 100\,\% \quad (6)$$

2.8.5 | Total oil recovery and content

Powder samples (except CW13 and CW14) were reconstituted using ultrapure water to obtain a similar solid content with those of the corresponding emulsions. The oil was then extracted from the emulsions using the method described in Section 2.3. Due to limited solubility in water, oil extraction from samples CW13 and CW14 was conducted using *n*-hexane directly. The powder (6 g) was dispersed in 40 ml *n*-hexane with constant stirring (300 rpm for 12 h at room temperature). The total oil recovery and content were calculated according to Equations (7) and (8).

$$\text{Total oil recovery}\,(\%) = \frac{\text{extracted oil}\,(\text{g})}{\text{theoretical total oil}\,(\text{g})} \times 100\,\% \quad (7)$$

$$\text{Total oil concentration}\,(\%) = \frac{\text{extracted oil}\,(\text{g})}{\text{mass of the powder sample}\,(\text{g})} \times 100\,\% \quad (8)$$

2.8.6 | Microencapsulation efficiency

The microencapsulation efficiency (ME) was calculated according to Equation 9 (Eratte et al., 2014).

$$\text{ME}\,(\%) = \frac{\text{theoretical total oil}\,(\text{g}) - \text{surface oil}\,(\text{g})}{\text{theoretical total oil}\,(\text{g})} \times 100\,\% \quad (9)$$

2.9 | Oxidative stability during storage

The oxidative stability of emulsions and microencapsulated powders were evaluated by an accelerated storage trial. For emulsions, 400 ml of freshly prepared emulsion was incubated at 55°C without light in a 500 ml glass bottle. Sampling was conducted at 0, 5, 10, 15, and 20 days for the determination of PV, AV, and antioxidant capacity. For powders, a total of 6 g powder sample was stored in a small glass bottle at 55°C without light. Sampling was conducted at 0, 2, 6, 10, 15, and 20 days for the determination of PV, AV, and antioxidant capacity. The samples at 0, 10, and 20 days were obtained for determinations of linoleic acid and linolenic acid content.

2.10 | Statistical analysis

All experiments and analyses were performed in triplicate. Statistical analysis was conducted using the SPSS 23 software (IBM, New York, NY, USA). One-way ANOVA and Duncan's test were conducted to compare the differences in mean values. Data were considered as significantly different at $p < .05$.

3 | RESULTS AND DISCUSSION

3.1 | Characterization of the O/W emulsions

3.1.1 | Droplet size and distribution

The droplet sizes of the emulsions are shown in Table 1. The droplet sizes of PO-containing emulsions stabilized by WPI/GA, WPI/MD, and OSA-starch were in a range of 214.6 to 292.1 nm, which was significantly ($p < .05$) smaller than those structured by WPI/GA via the complex coacervation process (i.e., 2349.0 nm for CWG13 and 1002.3 nm for CWG14 samples). The smallest droplet size was observed for the WG14 emulsion, which was likely due to the good emulsifying property of GA. This finding is supported by Buffo et al. (2001), who reported that higher content of GA in emulsions would result in better emulsification. Comparing the emulsions containing similar materials but with different core-to-wall ratios, it was obvious that the emulsions with the ratio of 1:3 have a bigger droplet size than those with the ratio of 1:4.

The samples containing WPI/MD have significantly larger droplet sizes ($p < .05$) than those prepared from WPI/GA (Table 1). This agrees with the results of a previous study on microencapsulation of linoleic acid using similar wall materials (Minemoto et al., 2002). These results indicated that GA has a better emulsifying property than MD. One possible reason is the presence of proteineous residues in GA can closely linked to the polymer chains of carbohydrate through molecular interactions, and the complex formed can attach to the surface of oil droplets rapidly during the homogenization process (Dickinson, 2003). Comparing the droplet size of the emulsions, the OSA-starch emulsions have a significant ($p < .05$) larger droplet size than those formed by the WPI/GA and WPI/MD (Table 1). The results also showed that when the content of OSA-starch increased in the emulsion formulation, the droplet size became significant ($p < .05$) smaller. This observation was reported in a previous research involving sunflower oil emulsions stabilized by OSA-starch (Dokić et al., 2012). The phenomenon could be attributed to the macromolecular structure of OSA-starch and its viscosity in water phase. With the increase in OSA-starch content in the emulsion formulation, the viscosity of the water phase would also increase as starch-bound water and gave a thickening effect. This could slow down the mobility of the droplets, and thus reducing the coalescence between droplets. Consequently, a smaller droplet size of emulsion was obtained.

TABLE 1 The average droplet size, PDI, and Zeta-potential of emulsions

	Droplet size (nm)	PDI	Zeta-potential (mV)
CWG13	2349.0 ± 308.4^{b}	1.000 ± 0.000^{c}	-15.10 ± 0.00^{ef}
CWG14	1002.3 ± 95.5^{c}	0.890 ± 0.190^{c}	-13.17 ± 0.51^{f}
WG13	232.1 ± 3.4^{aB}	0.300 ± 0.031^{abC}	-41.57 ± 4.00^{cC}
WG14	214.6 ± 4.7^{aA}	0.345 ± 0.034^{bD}	-39.50 ± 0.52^{cC}
WM13	242.3 ± 4.6^{aC}	0.270 ± 0.009^{abBC}	-49.33 ± 0.51^{bB}
WM14	236.6 ± 4.1^{aBC}	0.286 ± 0.007^{abC}	-57.20 ± 0.61^{aA}
OSA13	292.1 ± 2.8^{aE}	0.191 ± 0.020^{aA}	-19.10 ± 0.69^{dD}
OSA14	282.9 ± 1.5^{aD}	0.236 ± 0.009^{abB}	-16.60 ± 0.30^{deD}

Note: CWG13 and CWG14 refer to emulsions prepared via complex coacervation with WPI/GA as wall material and core-to-wall ratio of 1:3 and 1:4, respectively; WG13 and WG14 refer to emulsion prepared via homogenization with WPI/GA as wall materials and core-to-wall ratio of 1:3 and 1:4, respectively; WM13 and WM14 refer to emulsion prepared via homogenization with WPI/MD as wall materials and core-to-wall ratio of 1:3 and 1:4, respectively; OSA13 and OSA14 refer to emulsion prepared via homogenization with OSA as wall material and the core-to-wall ratio of 1:3 and 1:4, respectively. All samples contain 15% total solids. Different lowercase letters (a, b, c, d, e, f) indicate significant differences ($p < .05$) in a column for all emulsion samples. Different uppercase letters (A, B, C, D, E) indicate significant differences ($p < .05$) in a column for all samples except those prepared via complex coacervation.

3.1.2 | PDI and zeta-potential

The PDI of emulsions prepared with complex coacervation (CWG13 and CWG14) was significantly ($p < .05$) larger than other emulsions (Table 1). This is expected as insoluble complexes were formed due to electrostatic interactions between WPI and GA, leading to phase separation. The PDI of other emulsions (i.e., WG13, WG14, WM13, WM14, OSA13, and OSA14) was in a range of 0.191 to 0.345 with significant ($p < .05$) differences among some samples. The OSA13 emulsion showed the lowest PDI value (0.191 ± 0.020) among the samples, implying the smallest droplet size distribution for this sample. According to literature, a PDI value in the range of 0.1 to 0.25 is considered a narrow size distribution (Tantra et al., 2010). For samples having similar wall materials, emulsions with a core-to-wall ratio of 1:4 were found to have a higher PDI than those with a 1:3 ratio. Comparing samples with different wall materials, emulsions produced with OSA-starch have significant ($p < .05$) lower PDI values than other emulsions.

The emulsions' stability depends on the strength of interaction between the droplets, which can be determined by the electric charge on the droplet surface or zeta potential. The emulsions prepared with WPI/MD showed the highest absolute value of zeta-potential, followed by the WPI/GA and OSA samples (Table 1). An absolute value of zeta-potential >30 mV could trigger the repulsive forces between the droplets to prevent them from aggregating, thus, improving the physical stability of the emulsions (Tantra et al., 2010). Overall, the results (Table 1) indicated that the droplet size, PDI, and zeta-potential of emulsions were affected by wall material type.

3.1.3 | Oxidative stability of O/W PO emulsions

Oxidative stability of the PO emulsions plays a significant role in determining the quality of the microcapsules. Two major oxidation reactions can occur in the food system, that is, auto-oxidation and photo-oxidation. Auto-oxidation commonly happens in the presence of oxygen, especially with light, heat, or metal ions. To investigate the emulsion stability, the PV, PAV, and antioxidant capacity were measured (Figure 1).

3.1.3.1 | *Peroxide value*

Peroxide value (PV), an indicator of the initial stage of oxidative changes, is commonly used to determine the continuous formation of hydroperoxides to assess oil quality. The initial PVs of all emulsions were around 6 meq/kg oil with no significant differences among samples. This value is acceptable as fresh vegetable oils generally have PV values of less than 10 meq/kg oil. The PV of emulsions showed an overall increasing trend during the 15 days of storage at 55°C (Figure 1a,b). This indicated the formation of hydroperoxides from the unsaturated fatty acids due to primary lipid oxidation at a high temperature. However, the emulsions containing WPI/GA and WPI/MD experienced a rapid increase in PV in the first 6 days, followed by a slow decrease. The hydroperoxides formed during primary oxidation were unstable and highly susceptible to break down into secondary oxidation products, resulting in decreased PV at the end (Kaleem et al., 2015).

The emulsions prepared with WPI/MD showed the highest increase rate of PV at the first days of storage, reaching 90 meq/kg oil for WM13 and 73 meq/kg oil for WM14 samples at Day 6 (Figure 1a,b). On the other hand, the emulsions produced with WPI/

GA (WG13 and WG14) achieved the maximum PV (65 and 60 meq/kg oil, respectively) at Day 10. Compared to the emulsions containing WPI, samples with OSA-starch showed a slower increase in PV, indicating better oxidative stability. This phenomenon could be due to the deterioration of protein stabilization induced by several factors such as high pressure, shear stress, and high temperature during homogenization (Floury et al., 2000). Figure 1a,b shows that the PV changes in emulsions prepared by WPI/GA via complex coacervation (i.e., CWG13 and CWG14) resembled the trends of the OSA-starch stabilized emulsions (i.e., OSA13 and OSA14). This suggested that the complex coacervation process is favorable to maintaining the oxidative stability of emulsions. In addition, the emulsions with a core-to-wall ratio of 1:3 showed higher PVs than samples with a 1:4 ratio, mostly related to higher PO content and lower PDI value in those samples.

3.1.3.2 | *p-anisidine value*

Auto-oxidation generates a series of breakdown products, starting with primary oxidation products as reflected by PV, followed by secondary products (e.g., carbonyls, aldehydes, and trienes) and tertiary products. PAV is commonly used to assess the secondary oxidation of oils, which is mainly imputable to aldehydes and ketones, principally 2,4-dienals and 2-alkenals (Li et al., 2016).

Figure 1c,d illustrates the evolution of the secondary oxidation products in the emulsions during a 15-day storage trial. The PAVs of all emulsions were approximately 3 at day 0 ($p > .05$). Similar to the trend of primary oxidation (Figure 1a,b), the PAV of PO in all the emulsion samples increased over time but with a longer induction period. This was because the conversion of primary to secondary oxidation products is time-dependent. Moreover, the PAVs increased at different rates for all emulsions, depending on the wall material used. Overall, the trend for both core-to-wall ratios were: OSA-starch < WPI/GA prepared via coacervation < WPI/GA < WPI/MD. The PAVs of emulsions prepared with OSA-starch were kept relatively constant before Day 6, while other emulsions significantly increased ($p < .05$) from Day 2. The results indicated that emulsions prepared with OSA-starch and WPI/GA via coacervation could have a better oxidative stability than the samples stabilized by either WPI/GA or WPI/MD.

3.1.3.3 | *Antioxidant capacity*

Similar to PV and PAV, the antioxidant capacity evaluated via DPPH assay was used to indicate the oxidative stability of emulsions during storage. Our results have clearly shown that the antioxidant capacities of all emulsions decreased over time, and the degradation rates varied with the type of wall materials applied (Figure 1e,f). The initial antioxidant capacities of emulsions with a core-to-wall ratio of 1:3 ranged from 9 to 10 mM TE/L, while samples with the ratio of 1:4 were about 8 mM TE/L. After 15 days of storage, the emulsions produced with WPI/MD lost about 90%–95% of the DPPH antioxidant capacity, while samples prepared with OSA-starch showed a lower loss of around 68%–72%. The samples prepared with WPI/GA and WPI/GA via complex coacervation showed a similar loss rate of 17–23% for both core-to-wall ratios. Current results indicated that emulsions prepared by OSA-starch had better antioxidant stability than the other samples, which agrees with the PV and PAV results (Figure 1a–d). To elaborate this phenomenon, the emulsifying properties of wall materials and the encapsulation efficiency of PO were comprehensively investigated in Section 3.2.

3.2 | Characterization of the spray-dried PO powders

To improve the storage stability of PO, the emulsions were spray-dried into powders. The critical physicochemical properties, including morphology, moisture content, water activity, density, and encapsulation efficiency were investigated to evaluate the quality of the encapsulated powders. Considering the overall oxidative stability (Figure 1), the following emulsion samples with a total solid content of 15% (w/w) were selected for drying: WG14, CWG14, WM14, OSA13, and OSA14. An extra OSA14 sample with a higher total solid content of 30% (w/w) (OSA14-30) was also included as a comparison to the OSA14 sample.

3.2.1 | Microstructures

The microcapsules produced were varied in particle size and morphology (Figure 2). All samples were observed to have irregular spherical shapes with different surface features. The WG13, CWG13, and WM13 samples have a relatively smooth surface with no apparent cracks (Figure 2a–c). All these samples contain WPI as one of the wall materials. Similar morphological features of particles containing WPI were previously observed (Lu et al., 2021; Zhang, Peng, et al., 2020). Looking at the microcapsules containing WPI, the WM13 sample showed more broken surfaces (Figure 2c) than the WG13 and CWG13 samples, indicating a weaker encapsulating property of WPI/MD as wall materials for PO encapsulation. This is confirmed by the low encapsulation efficiency of this sample (Table 3). Comparing the microcapsules obtained from different wall materials, the microcapsules produced with OSA-starch exhibited a severely wrinkled surface with noticeable bulges and indentations (Figure 2d,e). This is thought to be a characteristic feature for spray-dried microcapsule as similar observations were noted for the microcapsules produced by spray drying microencapsulation of CoQ10 in olive oil (Zhao & Tang, 2016), CoQ10 and vitamin E (Huang et al., 2019), and algal oil (Wang et al., 2020).

3.2.2 | Water activity and moisture content

The water activity (a_w) and moisture content are two critical indices related to the shelf-life of spray-dried powders. The a_w of powders ranged from 0.209 to 0.297 (Table 2), with a significant difference ($p < .05$) between samples. The OSA14-30 powder showed the

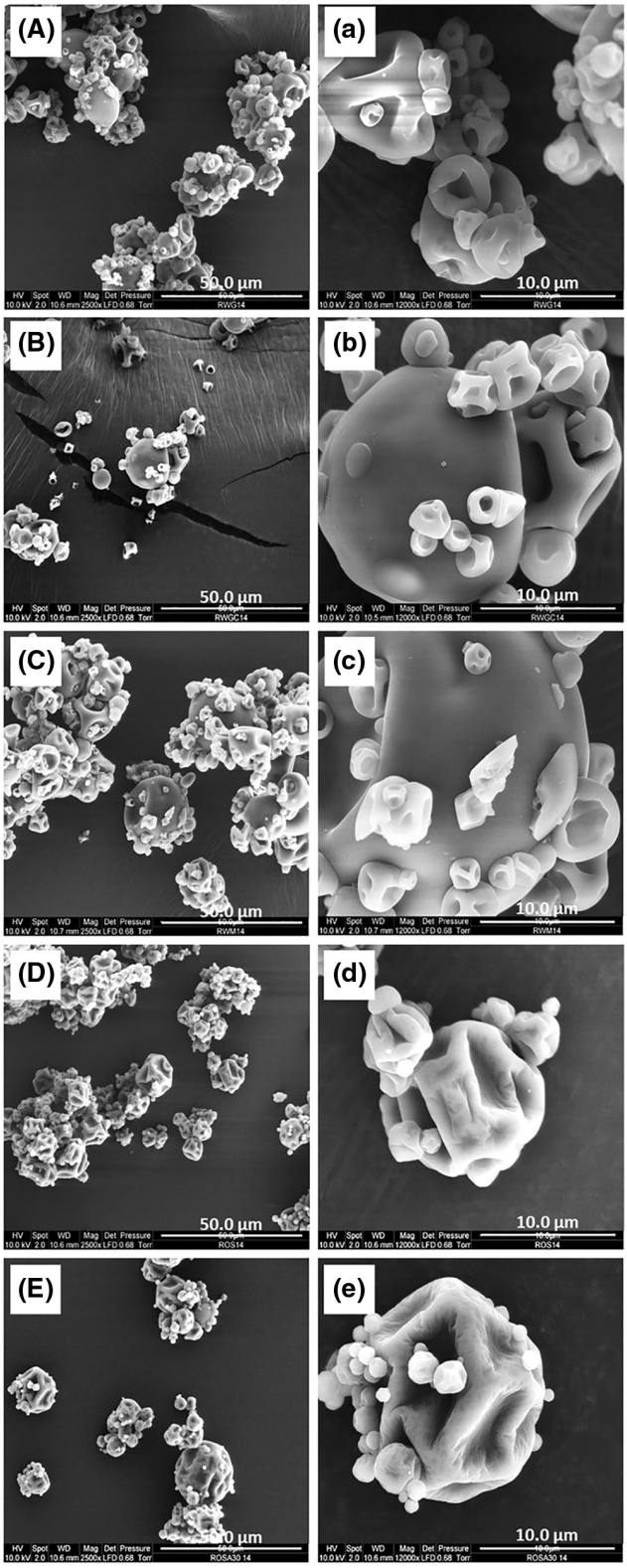

FIGURE 2 SEM micrographs showing microstructures of PO microcapsules containing different wall materials. All the microcapsules in the same raw have similar wall material compositions (A & a for WG14; B & b for CWG14; C & c for WM14; D & d for OSA14; E & e for OSA14-30) but at different magnifications of 2500× and 12,000×.

lowest a_w (0.209) and moisture content (4.33%) among all samples. Noteworthy, since the food system with an $a_w < 0.3$ is generally considered as safe from microbial deterioration and undesirable changes (Zhang, Zhang, et al., 2020), all encapsulated PO powders were microbiologically and chemically stable according to their a_w values (Table 2). Moreover, the moisture content of all powders ranged from 4.330 to 8.923%, with significant ($p < .05$) differences among samples (Table 2). These indicated that both a_w and moisture content of powders obtained were affected by the type of wall materials used in the current study. Similar results were reported on the spray-dried powders of CoQ10 and vitamin E (Huang et al., 2019), noni juice (Zhang, Ada Khoo, et al., 2020), mandarin juice (Chen et al., 2021), and *Lactobacillus rhamnosus* (Liao et al., 2021) comprising similar wall materials.

3.2.3 | Density

The bulk and tapped density (ρB and ρT) of spray-dried powders are crucial parameters related to the packaging and transportation cost. The Carr's index (CI) is used as an indicator for evaluating powder flowability. The ρB, ρT, and CI of all samples are shown in Table 2.

The OSA14-30 powder was found to have the highest ρB among the six samples ($p < .05$), followed by the OSA13 and OSA14 powders, while the CWG14 powder showed the lowest ρB. A similar tendency was observed on the ρT of powders ($p < .05$). The difference in ρB and ρT of samples could be due to the variation in particle size and morphology of microcapsules produced with OSA-starch and other wall materials including WPI, MD, and GA (Zhang, Khoo, et al., 2020). From Table 2, all CI values are above 25%, indicating that the microcapsules produced have a cohesive nature. It is noted that the powders produced with OSA-starch at 15% solid content (OSA13 and OSA14) showed significantly lower values than other samples, closer to 25%. This implied that microcapsules produced with OSA-starch have a relatively better flowability than those produced with WPI/MD, WPI/GA, and WPI/GA via complex coacervation.

3.2.4 | Total oil recovery and encapsulation efficiency

Encapsulation efficiency (EE) evaluates the amount of oil entrapped into the microcapsules structured by the wall materials. The EE of powders ranged from 87.43% to 98.18%, and the total oil recovery varied from 85.87% to 94.97% (Table 3). The overall performance of the wall materials based on EE is as follows: OSA-starch > WPI/GA via complex coacervation > WPI/GA > WPI/MD. This meant that OSA-starch is a better wall material for spray drying microencapsulation of PO than the other wall materials applied in this study. Previous research has reported that OSA-starch-based microcapsules displayed more impressive entrapping property and EE for oil compared to WPI, MD, and GA (Wang, Yuan, & Yue, 2015). This phenomenon could be

TABLE 2 The physicochemical properties of microcapsules

Sample	Water activity	Moisture content (%)	Bulk density (g/cm^3)	Tapped density (g/cm^3)	Carr's index (%)
WG14	0.231 ±0.002^b	5.957 ±0.053^d	0.240 ±0.001^c	0.348 ±0.001^b	31.01 ±0.25^b
CWG14	0.283 ±0.002^d	5.663 ±0.079^c	0.163 ±0.000^a	0.302 ±0.000^a	45.94 ±0.12^e
WM14	0.281 ±0.002^d	8.923 ±0.062^f	0.229 ±0.001^b	0.354 ±0.001^c	35.06 ±0.16^d
OSA14	0.297 ±0.002^e	5.363 ±0.012^b	0.293 ±0.001^d	0.404 ±0.001^d	26.45 ±0.24^a
OSA13	0.252 ±0.003^c	6.213 ±0.090^e	0.312 ±0.000^e	0.422 ±0.004^e	26.46 ±0.15^a
OSA14-30	0.209 ±0.000^a	4.330 ±0.091^a	0.335 ±0.000^f	0.536 ±0.005^f	34.61 ±0.21^c

Note: Values with a different letter are significantly different ($p < .05$) from each other; Mean ± SD, $n = 3$.

TABLE 3 Total oil recovery and encapsulation efficiency of microcapsules

Sample	Total oil recovery (%, w/w)	Encapsulation efficiency (%, w/w)
WG14	85.87 ±0.25^a	88.76 ±0.87^a
CWG14	90.09 ±0.23^b	93.37 ±0.62^b
WM14	86.04 ±0.35^a	87.43 ±0.82^a
OSA14	91.51 ±0.89^c	96.00 ±0.96^c
OSA13	93.05 ±0.63^d	95.86 ±0.80^c
OSA14-30	94.97 ±0.07^e	98.18 ±0.14^d

Note: Values with a different letter are significantly different ($p < .05$) from each other; Mean ± SD, $n = 3$.

attributed to the excellent emulsification capacity of OSA-starch. OSA-starch's high molecular weight (MW) engenders the formation of thicker film than emulsifiers with lower MW, leading to efficient emulsification (Sharif et al., 2017). Comparing the two powders with OSA-starch, the sample with a higher total solid content (OSA14-30) was found to have a higher EE and total oil recovery ($p < .05$), as expected. For drying droplets with similar wall material, droplets with a higher solid content can form surface crust earlier than those with lower solid content (Zhang, Fu, et al., 2019; Zhang, Quek, et al., 2019). Early crust formation does not favor oil diffusion from inside to the surface of semi-dried particles, resulting in a higher EE and total oil recovery. This finding is supported by previous research investigating surface formation phenomena of particles containing DHA and OSA-starch by single droplet drying experiments (Wang, Che, et al., 2015). The results (Table 3) also indicated that coacervation increased the EE of PO in samples with similar wall composition (93.37 ± 0.62% vs. 88.76 ± 0.87%).

3.2.5 | Stability of the spray-dried PO powder

Spray drying is generally applied for oil microencapsulation, aiming to reduce oxidative deterioration. However, oil oxidation may still occur during storage. The oxidative stability of the PO powders was invesitgated by analyzing the PV, AV, and DPPH antioxidant capacity and retention of the primary fatty acids in PO through a 20-day storage trial at 55°C.

The PVs and AVs of all powders gradually increased during storage in the following trend, according to wall materials: OSA-starch > WPI/GA via coacervation > WPI/GA > WPI/MD (Figure 3a,b). The trend is similar to the PV and AV changes in the corresponding emulsions (Figure 1) and the EE of powders (Table 3). Once again, microcapsules produced with OSA-starch were found to have a significantly lower rate for primary and secondary oxidation than other samples ($p < .05$, Figure 3a,b). Samples with lower EE would have more unencapsulated PO remained on the microcapsule surface, which were in more accessible contact with oxygen, thus, progressing lipid oxidation. It is noted that the OSA14-30 sample, which has a higher solid content of 30%, showed a slower oxidation rate. This is mainly due to its higher EE and lower moisture content than other powders (Table 3). The antioxidant capacities of powders were gradually decreased during the storage (Figure 3c), showing a similar tendency to the antioxidant capacity of the corresponding emulsions as discussed in Section 3.1.3.3 (Figure 1).

Comparing the results, the PVs of the emulsions increased more rapidly than the microcapsules at the same period. For example, at Day-6, PV of OSA14 and WM14 was 29% and 73%, respectively (Figure 1b), while the PVs for the corresponding microcapsules were 24% (OSA14) and 31% (WM14) (Figure 3a). Similar results were observed for the PAVs of the emulsion and powder samples during storage (Figures 1d and 3b). The trends also applied to the antioxidant capacity of powders especially in the first 10 days of storage. At Day-10, about 70% of antioxidant capacity remained in the powder samples (i.e., OSA14, WG14, CWG14, and WM14) while that of the emulsions varied from 13% (WM14) to 42% (OSA14). These results indicated that converting emulsions into a dry format could effectively slow down the oxidation rate and decrease the loss of antioxidant capacity in PO during storage.

Consistent with the literature (Choi et al., 2020), the primary fatty acids in the PO used in the current study were identified as palmitic, stearic, oleic, linoleic acid (LA), and linolenic acid (ALA) (Table A1), of which LA and ALA are two essential fatty acids that cause oxidation. From the present study, all the powders were observed to lose only 0%–5% of LA and ALA after spray drying (Day-0), indicating the successful stabilization of LA and ALA during the spray drying microencapsulation. The results were supported by a previous study on spray drying of peony seed oil (Wang et al., 2018). After 20 days of accelerated storage at 55°C, the LA and ALA contents in the

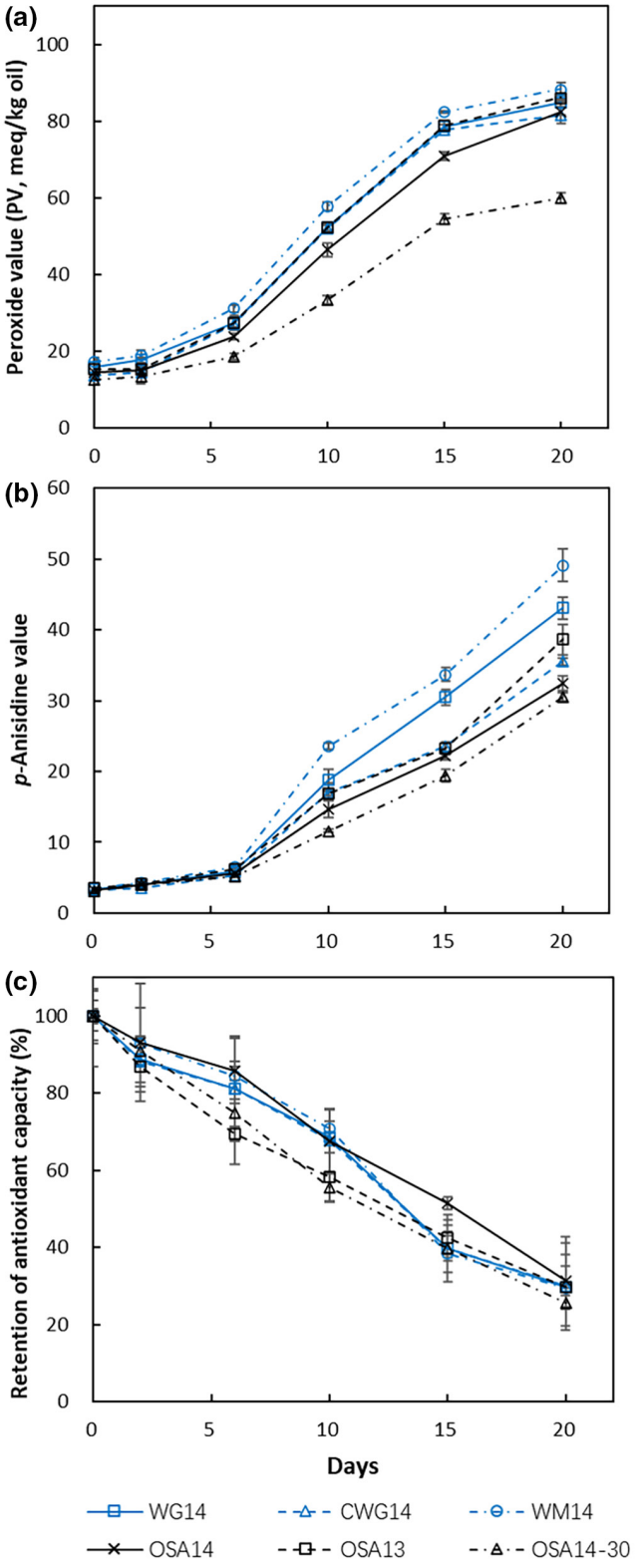

FIGURE 3 Changes in PV (a), AV (b), and antioxidant capacity (c) in microcapsules during storage.

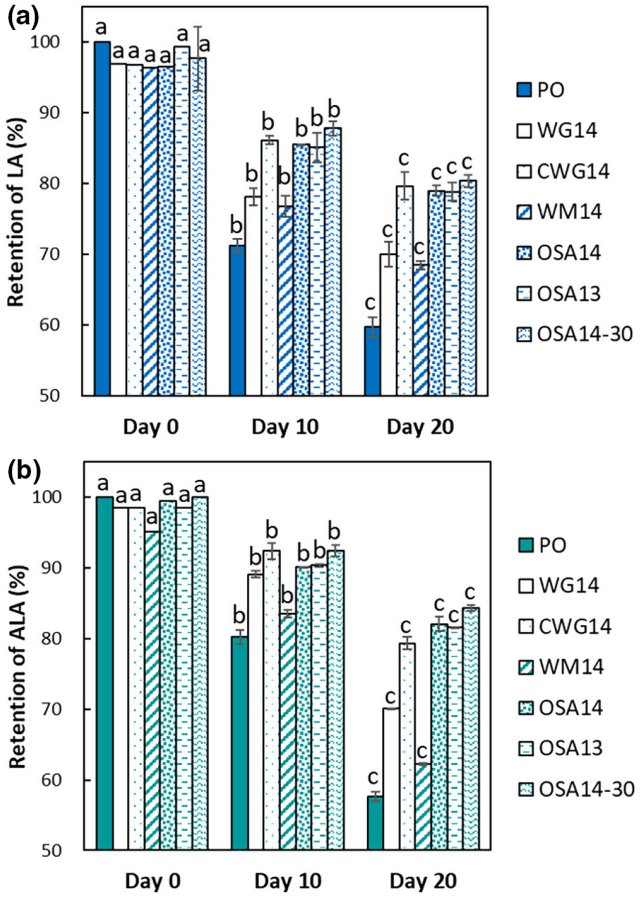

FIGURE 4 Retention of linoleic acid (a) and linolenic acid (b) in microcapsules during storage. The bars with different letters for each sample at different storage stages are significantly different ($p < .05$).

powders have significantly decreased ($p < .05$, Figure 4). Among the samples, the powders produced with OSA-starch and WPI/GA via coacervation were observed to have significantly higher retention of LA (about 80%) than other powders (Figure 4a). The control PO without microencapsulation has the lowest LA retention of >60% after storage. A similar trend was observed for ALA retention in the powders (Figure 4b). These findings indicated that spray drying microencapsulation of PO using OSA-starch and WPI/GA via coacervation could efficiently improve the retention of unsaturated fatty acids during storage. As discussed above, the phenomenon could be related to the high EE of powders produced with OSA-starch and WPI/GA via complex coacervation.

4 | CONCLUSION

This study investigated the microencapsulation of PO into emulsion and microcapsule formats using carbohydrates and proteins as wall materials. The physicochemical properties and oxidative stability of the emulsions and spray-dried powders affected by the wall materials were examined. Overall, the findings suggest that OSA-starch could be a promising wall material for microencapsulating PO in both emulsions and microcapsules, as it produced samples with better PDI, encapsulation efficiency, and oxidative stability than the other samples stabilized by WPI/MD, WPI/GA,

and WPI/GA via complex coacervation. Spray drying microencapsulation could effectively improve the oxidative stability and loss of antioxidant capacity of PO during storage. In addition, the primary unsaturated fatty acids in PO (LA and ALA) were well-protected in the powders after spray drying and during storage. On the other hand, complex coacervation could enhance the encapsulation efficiency and improve the oxidative stability of the emulsion and microcapsule, but it increases the droplet size of the emulsion.

AUTHOR CONTRIBUTIONS

Chuang Zhang: Writing - original draft; Writing - review & editing; Formal analysis. **Wenting Zhou:** Investigation; Conceptualization; Methodology; Writing - original draft. **Jiqian Xiang:** Resources. **Hong Chen:** Resources; Investigation. **Siew Young Quek:** Conceptualization; Methodology; Supervision; Writing - review & editing.

ACKNOWLEDGMENTS

The authors acknowledge Enshi Academy of Agricultural Science and The University of Auckland for funding the research. Open access publishing facilitated by The University of Auckland, as part of the Wiley - The University of Auckland agreement via the Council of Australian University Librarians.

CONFLICT OF INTEREST

The authors have declared no conflicts of interest for this article.

DATA AVAILABILITY STATEMENT

Research data are not shared.

ORCID

Chuang Zhang https://orcid.org/0000-0002-5502-5294

REFERENCES

Anderson, B. M., & Ma, D. W. (2009). Are all n-3 polyunsaturated fatty acids created equal? *Lipids in Health and Disease*, *8*(1), 1–20.

AOCS. (1998). AOCS. Official Method Cd 8-53. Peroxide value. American Oil Chemists' Society (AOCS).

AOCS. (2009). *p*-Anisidine value. Official Method Cd 18-90. In *Official methods and recommended practices of the American Oil Chemists' Society*. American Oil Chemists' Society (AOCS).

Bae, E., & Lee, S. (2008). Microencapsulation of avocado oil by spray drying using whey protein and maltodextrin. *Journal of Microencapsulation*, *25*(8), 549–560.

Buffo, R., Reineccius, G., & Oehlert, G. (2001). Factors affecting the emulsifying and rheological properties of gum acacia in beverage emulsions. *Food Hydrocolloids*, *15*(1), 53–66.

Chen, L., Li, R., Jiang, Z., & Tan, J. (2013). Comparative study on properties of the microencapsule of perilla oil entrapped with different microencapsulation methods. *Science and Technology of Food Industry*, *34*(20), 176–180 (In Chinese).

Chen, L., Li, R., Zhang, L., & Jiang, Z. (2015). Preparation and performance studies on the microencapsule of perilla oil entrapped with complex coacervation. *Science and Technology of Food Industry*, *36*(03), 232–238 (In Chinese).

Chen, X., Ting, J. L. H., Peng, Y., Tangjaidee, P., Zhu, Y., Li, Q., Shan, Y., & Quek, S. Y. (2021). Comparing three types of mandarin powders prepared via microfluidic-jet spray drying: Physical properties, phenolic retention and volatile profiling. *Food*, *10*(1), 123.

Chen, Z. G., Bishop, K. S., Tanambell, H., Buchanan, P., Smith, C., & Quek, S. Y. (2019). Characterization of the bioactivities of an ethanol extract and some of its constituents from the New Zealand native mushroom Hericium *novae-zealandiae*. *Food & Function*, *10*(10), 6633–6643.

Choi, H. J., Song, B. R., Kim, J. E., Bae, S. J., Choi, Y. J., Lee, S. J., Gong, J. E., Lee, H. S., Lee, C. Y., Kim, B. H., & Hwang, D. Y. (2020). Therapeutic effects of cold-pressed perilla oil mainly consisting of linolenic acid, oleic acid and linoleic acid on UV-induced photoaging in NHDF Cells and SKH-1 hairless mice. *Molecules*, *25*(4), 989.

Dickinson, E. (2003). Hydrocolloids at interfaces and the influence on the properties of dispersed systems. *Food Hydrocolloids*, *17*(1), 25–39.

Dokić, L., Krstonošić, V., & Nikolić, I. (2012). Physicochemical characteristics and stability of oil-in-water emulsions stabilized by OSA starch. *Food Hydrocolloids*, *29*(1), 185–192.

Eratte, D., Wang, B., Dowling, K., Barrow, C. J., & Adhikari, B. P. (2014). Complex coacervation with whey protein isolate and gum arabic for the microencapsulation of omega-3 rich tuna oil. *Food & Function*, *5*(11), 2743–2750.

Floury, J., Desrumaux, A., & Lardières, J. (2000). Effect of high-pressure homogenization on droplet size distributions and rheological properties of model oil-in-water emulsions. *Innovative Food Science & Emerging Technologies*, *1*(2), 127–134.

Gamazo-Vázquez, J., Garcıa-Falcón, M., & Simal-Gándara, J. (2003). Control of contamination of olive oil by sunflower seed oil in bottling plants by GC-MS of fatty acid methyl esters. *Food Control*, *14*(7), 463–467.

Gharsallaoui, A., Roudaut, G., Chambin, O., Voilley, A., & Saurel, R. (2007). Applications of spray-drying in microencapsulation of food ingredients: An overview. *Food Research International*, *40*(9), 1107–1121.

Han, L., Hou, Z., Wen, J., Wu, Y., Qian, Y., & Gong, S. (2016). Preparation and evaluation of high-loaded perilla seed oil by microencapsulation with different wall materials. *Science and Technology of Food Industry*, *08*, 167–170 (In Chinese).

Han, L., Lu, K., Zhou, S., Zhang, S., Xie, F., Qi, B., & Li, Y. (2021). Development of an oil-in-water emulsion stabilized by a black bean protein-based nanocomplex for co-delivery of quercetin and perilla oil. *LWT - Food Science and Technology*, *138*, 110644.

Hu, M., Xie, F., Zhang, S., Li, Y., & Qi, B. (2020). Homogenization pressure and soybean protein concentration impact the stability of perilla oil nanoemulsions. *Food Hydrocolloids*, *101*, 105575.

Huang, E., Quek, S. Y., Fu, N., Wu, W. D., & Chen, X. D. (2019). Co-encapsulation of coenzyme Q10 and vitamin E: a study of microcapsule formation and its relation to structure and functionalities using single droplet drying and micro-fluidic-jet spray drying. *Journal of Food Engineering*, *247*, 45–55.

Kaleem, A., Aziz, S., & Iqtedar, M. (2015). Investigating changes and effect of peroxide values in cooking oils subject to light and heat. *FUUAST Journal of Biology*, *5*(2), 191–196.

Katvi, S. R. (2005). *Investigating the lipid profiles of common New Zealand seafood* (Master Thesis). University of Auckland.

Kozłowska, M., Gruczyńska, E., Ścibisz, I., & Rudzińska, M. (2016). Fatty acids and sterols composition, and antioxidant activity of oils extracted from plant seeds. *Food Chemistry*, *213*, 450–456.

Li, J., Cai, W., Sun, D., & Liu, Y. (2016). A quick method for determining total polar compounds of frying oils using electric conductivity. *Food Analytical Methods*, *9*(5), 1444–1450.

Liao, Y., Hu, Y., Fu, N., Hu, J., Xiong, H., Chen, X. D., & Zhao, Q. (2021). Maillard conjugates of whey protein isolate-xylooligosaccharides for the microencapsulation of Lactobacillus rhamnosus: protective effects and stability during spray drying, storage and gastrointestinal digestion. *Food & Function*, *12*(9), 4034–4045.

Lu, W., Fu, N., Woo, M. W., & Chen, X. D. (2021). Exploring the interactions between Lactobacillus rhamnosus GG and whey protein

isolate for preservation of the viability of bacteria through spray drying. *Food & Function*, *12*(7), 2995–3008.

Minemoto, Y., Hakamata, K., Adachi, S., & Matsuno, R. (2002). Oxidation of linoleic acid encapsulated with gum arabic or maltodextrin by spray-drying. *Journal of Microencapsulation*, *19*(2), 181–189.

Sarabandi, K., Peighambardoust, S. H., Mahoonak, A. S., & Samaei, S. P. (2017). Effect of carrier types and compositions on the production yield, microstructure and physical characteristics of spray dried sour cherry juice concentrate. *Journal of Food Measurement and Characterization*, *11*(4), 1602–1612.

Sharif, H. R., Williams, P. A., Sharif, M. K., Khan, M. A., Majeed, H., Safdar, W., Shamoon, M., Shoaib, M., Haider, J., & Zhong, F. (2017). Influence of OSA-starch on the physico chemical characteristics of flax seed oil-eugenol nanoemulsions. *Food Hydrocolloids*, *66*, 365–377.

Swanson, D., Block, R., & Mousa, S. A. (2012). Omega-3 fatty acids EPA and DHA: health benefits throughout life. *Advances in Nutrition*, *3*(1), 1–7.

Tan, L., Chan, L., & Heng, P. (2005). Effect of oil loading on microspheres produced by spray drying. *Journal of Microencapsulation*, *22*(3), 253–259.

Tantra, R., Schulze, P., & Quincey, P. (2010). Effect of nanoparticle concentration on zeta-potential measurement results and reproducibility. *Particuology*, *8*(3), 279–285.

von Schacky, C. (2021). Importance of EPA and DHA blood levels in brain structure and function. *Nutrients*, *13*(4), 1074.

Wang, S., Hwang, H., Yoon, S., & Choe, E. (2010). Temperature dependence of autoxidation of perilla oil and tocopherol degradation. *Journal of Food Science*, *75*(6), C498–C505.

Wang, S., Shi, Y., & Han, L. (2018). Development and evaluation of microencapsulated peony seed oil prepared by spray drying: Oxidative stability and its release behavior during in-vitro digestion. *Journal of Food Engineering*, *231*, 1–9.

Wang, X., Yuan, Y., & Yue, T. (2015). The application of starch-based ingredients in flavor encapsulation. *Starch - Stärke*, *67*(3–4), 225–236.

Wang, Y., Che, L., Fu, N., Chen, X. D., & Selomulya, C. (2015). Surface formation phenomena of DHA-containing emulsion during convective droplet drying. *Journal of Food Engineering*, *150*, 50–61.

Wang, Y., Zheng, Z., Wang, K., Tang, C., Liu, Y., & Li, J. (2020). Prebiotic carbohydrates: Effect on physicochemical stability and solubility of algal oil nanoparticles. *Carbohydrate Polymers*, *228*, 115372.

Yi, T., Li, S. M., Fan, J. Y., Fan, L. L., Zhang, Z. F., Luo, P., Zhang, X. J., Wang, J. G., Zhu, L., & Zhao, Z.-Z. (2014). Comparative analysis of EPA and DHA in fish oil nutritional capsules by GC-MS. *Lipids in Health and Disease*, *13*(1), 1–6.

Zamani-Ghaleshahi, A., Rajabzadeh, G., Ezzatpanah, H., & Ghavami, M. (2020). Biopolymer coated nanoliposome as enhanced carrier system of perilla oil. *Food Biophysics*, *15*, 1–15.

Zhang, C., Ada Khoo, S. L., Chen, X. D., & Quek, S. Y. (2020). Microencapsulation of fermented noni juice via micro-fluidic-jet spray drying: Evaluation of powder properties and functionalities. *Powder Technology*, *361*, 995–1005.

Zhang, C., Fu, N., Quek, S. Y., Zhang, J., & Chen, X. D. (2019). Exploring the drying behaviors of microencapsulated noni juice using reaction engineering approach (REA) mathematical modelling. *Journal of Food Engineering*, *248*, 53–61.

Zhang, C., Khoo, S. L. A., Swedlund, P., Ogawa, Y., Shan, Y., & Quek, S. Y. (2020). Fabrication of spray-dried microcapsules containing noni juice using blends of maltodextrin and gum acacia: Physicochemical properties of powders and bioaccessibility of bioactives during *in vitro* digestion. *Food*, *9*(9), 1316.

Zhang, C., Quek, S. Y., Fu, N., Liu, B., Kilmartin, P. A., & Chen, X. D. (2019). A study on the structure formation and properties of noni juice microencapsulated with maltodextrin and gum acacia using single droplet drying. *Food Hydrocolloids*, *88*, 199–209.

Zhang, J., Zhang, C., Chen, X., & Quek, S. Y. (2020). Effect of spray drying on phenolic compounds of cranberry juice and their stability during storage. *Journal of Food Engineering*, *269*, 109744.

Zhang, Z. H., Peng, H., Woo, M. W., Zeng, X. A., Brennan, M., & Brennan, C. S. (2020). Preparation and characterization of whey protein isolate-chlorophyll microcapsules by spray drying: Effect of WPI ratios on the physicochemical and antioxidant properties. *Journal of Food Engineering*, *267*, 109729.

Zhao, X. H., & Tang, C. H. (2016). Spray-drying microencapsulation of CoQ10 in olive oil for enhanced water dispersion, stability and bioaccessibility: Influence of type of emulsifiers and/or wall materials. *Food Hydrocolloids*, *61*, 20–30.

SUPPORTING INFORMATION

Additional supporting information can be found online in the Supporting Information section at the end of this article.

How to cite this article: Zhang, C., Zhou, W., Xiang, J., Chen, H., & Quek, S. Y. (2022). Fabrication, characterization, and oxidative stability of perilla seed oil emulsions and microcapsules stabilized by protein and polysaccharides. *Journal of Food Processing and Preservation*, *00*, e16950. https://doi.org/10.1111/jfpp.16950